Computer vision-based analytical chemistry applied to determining iron in commercial pharmaceutical formulations

A. Solana-Altabella[a], M.H. Sánchez-Iranzo[a], J.I. Bueso-Bordils[a], L. Lahuerta-Zamora[a], A.M. Mellado-Romero[b,*]

[a] *Departamento de Farmacia, Universidad CEU-Cardenal Herrera, c/ Santiago Ramón y Cajal s/n, 46115 Alfara del Patriarca, Valencia, Spain.*

[b] *Instituto de Ciencia y Tecnología del Hormigón (ICITECH), Universitat Politècnica de València, Camino de Vera s/n, 46022 Valencia, Spain.*

ABSTRACT

Two different computer vision-based analytical chemistry (CVAC) methods were developed to quantify iron in the commercial pharmaceutical formulations Ferbisol® and Ferro sanol®. The methods involve using a digital camera or a desktop scanner to capture a digital image of a series of Fe^{2+} standard solutions and the unknown sample upon reaction with *o*-phenanthroline. The images are processed with appropriate software (e.g., the public domain programme ImageJ, from NIH) to obtain a numerical value (analytical signal) based on colour intensity. The fact that such a value is proportional to the analyte concentration allows one to construct a calibration graph from the standards and interpolate the value for the sample in order to determine its concentration. The results thus obtained were compared with those provided by a spectrophotometric method and the US Pharmacopoeia's recommended method. The differences never exceeded 2%. The two proposed methods are simple and inexpensive; also, they provide an effective instrumental alternative to spectrophotometric methods which can be especially beneficial in those cases where purchasing and maintaining a spectrophotometer is unaffordable.

Keywords:

CVAC, digital camera, desktop scanner, ImageJ, pharmaceutical analysis.

* Corresponding author.
E-mail address: amellado@cst.upv.es (A.M. Mellado-Romero)

1. Introduction

Iron plays a central role as an active site for proteins effecting O_2 and electron transfer in enzymes (oxidases, reductases and dehydrases) in the biosphere. In fact, iron is an essential element for oxygen transport and storage through haemoglobin and myoglobin in higher animals [1–3]. As such, this element is an essential ingredient of human diet deficiencies in which are the source of a number of diseases, particularly during childhood, adolescence and pregnancy [4]. Thus, an iron-deficient diet can lead to a medical condition known as "ferropenic anaemia". Correcting iron deficiencies entails using an effective iron supplement such as a multi-vitamin complex or a specific pharmaceutical formulation.

A number of methods currently exist for determining iron most of which are based on volumetric [5], potentiometric [6], anodic stripping voltametric [7], graphite-furnace [8] or flame atomic absorption [9], inductively coupled plasma atomic emission spectrometry or inductively coupled plasma mass spectrometry [10], fluorimetric [~~10,~~11] or chemiluminescence [12, 13] measurements.

Spectrophotometry is among the most simple, expeditious and inexpensive techniques for determining iron in a wide variety of samples. The process usually involves reacting the iron with a chromogenic chelating agent [14-24].

In this work, we used the well-known spectrophotometric method for iron (II) based on its reaction with *o*-phenanthroline (at pH 3.5 by adding sodium acetate) to form a reddish orange complex [25].

Keeping iron in its reduced state (Fe^{2+}) requires using an appropriate reductant such as hydroxylamine.

The resulting complex can be quantified spectrophotometrically by its absorbance at 508 nm.

The decreasing cost and increasing performance of digital imaging hardware and software have promoted the increasing use of digital photography in colorimetric qualitative and quantitative tests which have given rise to an increasingly popular new analytical technique called "computer vision-based analytical chemistry" (CVAC) [26].

Digital imaging devices (e.g. digital cameras, desktop scanners) use either of two types of sensors, namely: *Complementary Metal Oxide Semiconductors*

(CMOS) or *Charge Coupled Devices* (CCD). A CCD (or a CMOS) is an electronic device henceforward referred to as a “sensor” consisting of many cells called “pixels”. Each cell acts as a light-sensitive element and provides an electrical response to light; the combined responses of a sensor can be digitized and converted into an image [26-28].

A sensor consisting of 8-bit pixels can respond to $2^8 = 256$ different levels of grey from 0 (black) to 255 (white). Therefore, each pixel in a captured image can be assigned a value from 0 to 255 that can be used for calibration. This allows a digital imaging device to be used as an analytical detector to exploit the vast amount of information contained in a captured image [26].

The CVAC technique has been increasingly used in research laboratories and commercial laboratory equipment for more than two decades [26, 28-41]. Low-cost commercial digital cameras and scanners have been gradually incorporated into the analytical laboratory, where they are being increasingly used for forensic [42, 43], telemedicine [27, 48] and, obviously, analytical purposes [26, 44, 46, 47, 49, 50, 53-55].

Using a commercial digital camera in combination with the software ImageJ recently proved a simple, inexpensive choice for a variety of measurements [27, 45].

Webcams and mobile phone cameras have proved useful for chemical analysis [46, 47] and even for capturing and transferring the results of biological tests for glucose and proteins in telemedicine [48].

On the other hand, commercial scanners have been also used to develop colorimetric methods [49-53].

In line with previous works [54, 55], the proposed method uses digital images of series of standard solutions in combination with imaging software (ImageJ) to assign a numerical value for colour intensity. Such a value is proportional to the concentration of the standard and can be used for calibration. Our method is similar to the classical spectrophotometric method for the same purpose but has the advantage that it uses much more simple and inexpensive hardware (viz., a low-cost digital camera or a desktop scanner) and public domain —and hence free— software (ImageJ). The results are compared with those provided by the classical spectrophotometric method and the official, cerimetric method recommended by the US Pharmacopoeia [56].

2. Material and methods

2.1. General materials

All reagents used were analytical-grade and obtained from the following suppliers: Panreac (hydroxylamine hydrochloride), J.T. Baker (1 mol L^{-1} sulphuric acid, ammonium iron (II) sulphate hexahydrate (Mohr's salt)) and Scharlab (*o*-phenanthroline monohydrate, sodium acetate trihydrate). The cerimetric titration in the USP method was performed with 0.1 mol L^{-1} cerium (IV) sulphate (in 0.5 mol L^{-1} H_2SO_4) from Scharlab and 0.025 mol L^{-1} ferroin from J.T. Baker.

All solutions were prepared in water de-ionized to 18 MΩ·cm by reverse osmosis in a Sybron/Barnstead Nanopure apparatus furnished with a fibre filter of 0.2 μm pore size.

A standard solution containing 100 mg Fe(II) L^{-1} was prepared by dissolving 0.7 g of Mohr's salt in 1 mol L^{-1} H_2SO_4 and making to volume in a 1 L volumetric flask.

The solutions were transferred to the supports by using a 1000 μL Labopette® micropipette.

The commercial pharmaceutical formulations studied were Ferbisol® 100 mg (50 capsules; BIAL Industrial Farmacéutica, S.A.) and Ferro sanol® 100 mg (50 capsules; UCB Pharma, S.A.).

Absorbance measurements were obtained with a Spectronic Genesis 20 UV–Vis spectrophotometer. Each image was captured by placing a blank consisting of a strip of two-sided inkjet paper near the standards and support.

All images were processed by using the public domain software ImageJ for Windows developed by the National Institutes for Health and freely available for download at http://rsbweb.nih.gov/ij.

2.2. Material for capturing images with the digital camera

The standards and sample were held in a 11 × 9 cm white ceramic spot plate with 6 wells holding 3 mL each.

All photographs were taken with a Nikon Coolpix E995 digital camera. Lighting was provided by two pairs of Philips Master TL-D 36W/840 fluorescent tubes 1.5 m above the plate.

In order to avoid reflections of the fluorescent tubes on the plate and the associated artefacts in the images, the camera–plate combination was placed inside a 40 × 25 × 35 cm white methacrylate box (Fig. 1). Reflections off the inner walls of the box were avoided by using a diffusion screen consisting of a 420 × 520 mm piece of 60 g/m^2 ALBET white filter paper (LabScience code RM2504252). Also, the plate was placed on a piece of NE 30K black cardboard (A4, 108 g) from Hermanos Cebrián (Valencia, Spain) for increased contrast.

2.3. Material used for capturing images with the desktop scanner

The standard solutions and sample were placed in a TTP® Zellkultur Testplatte containing 24 wells holding 3 mL each.

Images were acquired with five different scanner models, namely: HP PSC 1510 All-in-one, HP Photosmart C3180, Brother DCP-J132W, HP ScanJet 3100 and Acer S2W 3300V.

2.4. General procedure

The experimental work was conducted under the typical chemical conditions of the well-known spectrophotometric method for determining Fe (II) with *o*-phenanthroline [25]. For this purpose, aliquots of 1–5 mL of the 100 mg Fe (II) L^{-1} standard and a blank (0 mL) were added to 100 mL volumetric flasks and successively supplied with 20 mL of water, 2 mL of hydroxylamine, 5 mL of *o*-phenanthroline and 5 mL of sodium acetate. These solutions were used to construct the calibration curve for iron (II).

The samples were prepared by adding the contents of 5 capsules of either pharmaceutical formulation to a beaker containing 250 mL of 1 mol L^{-1} sulphuric acid and stirring for 24 h. The resulting suspension was passed through paper filter and made to 500 mL with more sulphuric acid in a volumetric flask. A 250 μL aliquot of this solution was made to 100 mL in another flask and reacted identically with the standards.

The solutions were allowed to stand for 15 min, after which the concentration of iron in each was determined by digital imaging analysis.

2.5. Procedure with the digital camera

Obtaining useful images of the standards and samples required using an appropriate support in order to enhance the colour of the solutions without interference. A white ceramic plate with 3 mL wells proved suitable for this purpose as it allowed an image of all solutions (standards and sample) to be simultaneously obtained under identical lighting conditions.

Each plate well was filled with 3 mL of a standard solution containing a concentration within the linear calibration range (0.5 mg L^{-1}) and the plate photographed together with the white paper strip (Fig. 2a).

The camera was operated in the manual mode in order to avoid the potential influence of its automatically choosing its own settings. Because using flash could have resulted in unwanted reflections on the solution surfaces, all lighting was supplied by the laboratory's fluorescent strips. Also, any spurious signals due to reflections from other sources were minimized by placing the camera–plate combination inside a white methacrylate box lined with a diffusing screen on the inside.

These diffuse lighting conditions allowed the optimum F-stop and shutter speed to be selected in order to avoid under- and overexposure. The camera was attached to a static support and photographs were taken at F/6 and a shutter speed of 1/4 s.

2.6. Procedure with the scanner

Accurately capturing the colour of the standards and samples with the scanner required using a support consisting of a transparent microplate with 24 wells holding 3 mL of solution each. This support allowed an image of the standards and sample to be simultaneously obtained under identical lighting conditions.

Each microplate well was filled with 2 mL of a solution of the standards or sample containing concentrations within the linear calibration range (0–5 mg L^{-1}).

The amount of light reflected was maximized by placing a sheet of standard white paper on the microplate lid. Also, spurious reflections were avoided by covering the microplate with a piece of thick black cloth prior to scanning the microplate–paper strip combination (Fig. 2b).

2.7. Processing of images

All images were processed with the software ImageJ. A standardized image not dependent on the colour temperature of the source of light (namely, two fluorescent strips or the scanner lamp) was obtained by calibration with a strip of standard white paper.

The image was white-balanced by using an algorithm described elsewhere [27]. Each A>B>C operation involved selecting command B from menu A and then sub-command C from command B. First, the original image was split into three RGB images (*Image* > *Color* > *Split Channels*). Then a circular region of interest (ROI) in each RGB sub-image was selected with the drawing tool in the toolbar and placed on the white paper strip to measure its Mean Brightness (MB) by using the Histogram command (*Analyze* > *Histogram*). Next, on the assumption that the white paper strip reflected 80% of incident light in each channel (255 × 0.8 = 200), each RGB image was corrected by multiplying its brightness by 200/MB (*Process* > *Math* > *Multiply* and then enter 200/MB). The corrected sub-images were merged to obtain a new colour image mimicking one capture under ideally white lighting (*Image* > *Colour* > *Merge Channels*). This standard image was again split into RGB sub-images, that for the green channel being inverted and the level of neutral grey (NG) for each standard (or the sample) measured in the previously selected ROI (Fig. 2c).

The NG level for each standard or sample was taken to be the analytical signal and used to calculate the corresponding absorbance from [49]

$$\boldsymbol{Abs = \log \frac{NG}{255}}$$

which relates the absorbance of the analyte to its concentration.

2.8. Optimization procedure

The instrumental variables of the imaging process were optimized by using a univariate procedure. Each variable was examined at different values in order to establish that leading to the greatest sensitivity (highest slope of the calibration curve). For this purpose, iron (II) standards containing concentrations over the range 0–5 mg L^{-1} were used to obtain three consecutive images that were processed with ImageJ in order to construct three calibration curves with their respective slopes and coefficients of determination (r^2). The process was optimized in terms of the mean of both parameters and the standard deviation from the mean slope (N = 3).

3. Results and discussion

3.1. Digital camera

The initial conditions for the capturing process were established in previous work [55]. A comparison of the calibration curves for the green and blue colour channels — the red channel is useless owing to the colour of the iron complex— revealed that the former channel provided a more linear curve—at a similar deviation— and a greater slope. Therefore, the green channel was selected for subsequent measurements.

The influence of the exposure time was examined by using the camera’s greatest available aperture (F/3) and a focusing distance of 20 cm at shutter speeds from the highest (1/30 s) to the lowest (1/4 s); as revealed by the histograms, the former speed resulted in underexposure and the latter in overexposure (see Table 1). The slope increased with increasing exposure time; however, the coefficient of determination declined beyond 1/8 s, so a shutter speed of 1/15 s was selected as a trade-off for subsequent work.

In taking a photograph, the sensor can be exposed to identical amounts of light by using different combinations of aperture and exposure time. This phenomenon is called “reciprocity” and was used to identify the equivalent combinations of F/3 and a shutter speed of 1/15 s. As can be seen from Table 2, F/6 in combination with 1/4 s provided the best results in terms of slope and coefficient of determination, and were thus selected for subsequent work.

The influence of ROI size was examined at three different levels, namely: 20 000, 60 000 and 100 000 pixels. The optimum size was 60 000 pixels (see Table A in Supplementary material section).

3.2. Scanner

The performance of the scanner was compared with that of the digital camera by examining the potential influence of a number of instrumental and operational variables on the acquired images.

Initially, we used five different desktop scanners, all in the “auto” mode, in order to identify that providing the best results for the intended purpose. Each scanner was used to acquire images in the green and blue channels that were processed by using an ROI of a size equivalent to that of a plate well (2500 pixels for the Brother scanner and 4500 pixels for all others) or, alternatively, a smaller area (50 pixels) of uniform colour containing no apparent artefacts. Discrimination was based on the slope and coefficient of determination of the of the calibration curve. As can be seen from Table 3, the best trade-off between the two was provided by the Brother DCP-J132W scanner. This model has the added advantage that, because it is a combo system, it continues to operated even if the printer runs out of ink.

The influence of the volume of standard solution placed in each well was examined by using 1, 2 and 3 mL. A volume of 2 mL provided the best combination of slope and coefficient of determination (see Table B in Supplementary material section).

A comparison of the measurements on the green and blue channels revealed that the former resulted in smaller deviations, so it was selected for further work.
The optimum scanner allowed resolution, Gaussian blur, brightness and contrast, and the image format to be selected. This allowed us to examine the influence of these settings on the resulting calibration curves. Applying Gaussian blur led to similar coefficients of determination but reduced the slope of the curve, which excluded its use to improve the results. Also, using a small ROI (50 pixels) increased the slope (Table 4).

Scanner resolution ranged from 100 × 100 to 1200 × 1200 dpi. Resolution had no significant influence on the mean results (N = 3). This led us to select the lowest available resolution in order to obtain as small and expeditiously processed files as possible —in fact, the images obtained at the highest resolutions were too large for processing with ImageJ (see Table C in Supplementary material section).

As regards ROI size, a circle of 50 pixels led to a significantly greater slope than one of 2500 pixels, so NG was measured with the smaller size (see Table C in Supplementary material section).

The influence of the brightness and contrast settings on the calibration curve was examined by using a range of values in 10 unit steps. Negative values of the two settings led to underexposed, difficult to process images. Also, the large differences between using a brightness setting of +20 and one of +30 led us to test +25 as well; however, we chose to apply +30 to subsequent images as the optimum trade-off (see Tables D and E in Supplementary material section).

Regarding image compression, we tested the following choices: *standard baseline* (i.e., no compression, which is compatible with virtually any hardware and software), *optimized baseline* (compressed images) and *progressive* —which is useful for the Internet because images are viewed at a low resolution but downloaded at their actual resolution. All three formats led to similar results, so *optimized baseline* was selected in order to save space (see Table F in Supplementary material section).

3.3 Analytical figures of merit

3.3.1. Calibration curves. Limits of detection and quantitation.

The theoretical limits of detection (C_{LD}) and quantitation (C_{LQ}) were calculated as $3\sigma_b/m$ and $10\sigma_b/m$, respectively, σ_b being the standard deviation of the blank and *m* the slope of the calibration graph.

The empirical limit of detection was determined by using standard solutions containing 0–5 mg L^{-1} and assuming the limit to coincide with the point where the calibration curve ceased to be linear and the analytical signal was indistinguishable from the blank signal.

The theoretical and empirical limits are shown in Table 5.

3.3.2. Within-day and between-day reproducibility.

Within-day reproducibility was determined from images of five different sets of standard solutions containing 0–5 mg Fe L^{-1} that were obtained by the same operator using the same analytical equipment on the same day. The results are shown in Table 5.

Between-day reproducibility was determined similarly to within-day reproducibility except that the sets of standards were prepared on different days. The results are also shown in Table 5.

3.3.3. Determination of Fe (II) in real samples.

Two different commercial formulations of iron (II) (Ferbisol® and Ferro sanol®) were analysed with the four analytical methods studied, namely: analysis of digital images obtained with a photographic camera or a desktop scanner, spectrophotometry [25] and redox titrimetry (cerimetry) [56] —the last is the US Pharmacopoeia's recommended method and was used as reference for comparison. The manufacturers' stated content in iron of both formulations is 100 mg per capsule.

As can be seen from Table 6, all four methods proved suitable for determining iron in both formulations, with errors less than 2% in all cases and standard deviations only slightly higher than those of the officially endorsed method in the other three.

4. Conclusions

The two proposed methods exhibited good between-day reproducibility (RSD < 5% with $N = 5$) that was slightly higher with a photographic camera than with a scanner. The coefficients of the determination of the calibration curves were always higher than 0.995 and also slightly better with the camera than with the scanner.

The analytical results obtained with the two methods were comparable to those of the US Pharmacopoeia's recommended method for determining iron (II) in commercial pharmaceutical formulations (errors less than 2%) and even better than those for Ferbisol® provided by the classical spectrophotometric method.

Unlike a photographic camera, a scanner requires using no external lighting or diffusing screen.

The proposed methodology is simple and inexpensive. Thus, it uses a digital camera or desktop scanner connected to a computer, which is much more affordable equipment than a conventional spectrophotometer. Also, acquired images can be processed with user-friendly, free software (ImageJ, developed by the National Institutes for Health).

Given the current prevalence of increasingly sophisticated and expensive commercial instruments, the proposed methods provide a very interesting alternative for quantitative determinations in the absence of economic resources for purchasing and maintaining a conventional spectrophotometer.

5. Acknowledgements

This research did not receive any specific grant from funding agencies in the public, commercial or not-for-profit sectors.

6. References

[1] F. A. Cotton, G. Wilkinson, Advanced Inorganic Chemistry, 3ª ed. (1988), Wiley Interscience, New York.

[2] P. C. C. Oliveira, J.C. Masini, Sequential injection determination of iron (II) in antianemic pharmaceutical formulations with spectrophotometric detection, Anal. Lett. 34 (2001) 389-397. DOI: 10.1081/AL-100102581.

[3] D. Nichols, The Chemistry of Iron, Cobalt and Nickel (1973), Pergamon Press, Oxford.

[4] A. N. Araujo, J. Gracia, J.L.F.C. Lima, M. Poch, M. Lucia, M.F.S.Saraiva, Colorimetric determination of iron in infant fortified formulas by Sequential Injection Analysis, J. Fresenius, Anal. Chem. 357 (1997) 1153-1156. DOI: 10.1007/s002160050322.

[5] D. Tzur, V. Dosortzev, E. Kirowa-Eisner, Titration of low levels of Fe^{2+} with electrogenerated Ce^{4+}, Anal. Chim. Acta. 392 (1999) 307-318. DOI: 10.1016/S0003-2670(99)00226-3.

[6] W.H. Mahmoud, Iron Ion-Selective Electrodes for Direct Potentiometry and Potentiotitrimetry in Pharmaceuticals, Anal. Chim. Acta. 436 (2001) 199-206. DOI: 10.1016/S0003-2670(01)00892-3.

[7] S. Sundd, S.K. Prasad, A. Kumar, B.B. Prasad, Chelating resin-impregnated paper chromatography, applications to trace element collection of ferrous and ferric ions, and determination by differential pulse anodic stripping voltammetry, Talanta 41 (1994) 1943-1949. DOI: 10.1016/0039-9140(94)00153-7.

[8] P.C. Aleixo, J.A. Nobrega, Direct determination of iron and selenium in bovine milk by graphite furnace atomic absorption spectrometry, Food Chem. 83 (2003) 457-462. DOI: 10.1016/S0308-8146(03)00224-3.

[9] S. X. Li, N.S. Deng, Speciation analysis of iron in traditional Chinese medicine

by flame atomic absorption spectrometry, J. Pharm. Biol. Anal. 32 (2003) 51-57. DOI: 10.1016/S0731-7085(03)00024-4.

[10] V. Balaram, Recent advances in the determination of elemental impurities in pharmaceuticals – Status, challenges and moving frontiers, Trends in Analytical Chemistry 80 (2016) 83–95. DOI: 10.1016/j.trac.2016.02.001.

[11] G. Zhu, Z. Zhu, L. Qiu, A fluorometric method for the determination of iron(II) with fluorescein isothiocyanate and iodine, Anal. Sci. 18 (2002) 1059-1061. DOI: 10.2116/analsci.18.1059.

[12] P.L. Croot, P. Laan, Continuous shipboard determination of Fe(II) in polar waters using flow injection analysis with chemiluminescence detection, Anal. Chim. Acta. 466 (2002) 261-273. DOI: 10.1016/S0003-2670(02)00596-2.

[13] S. Hirata, H. Yoshihara, M. Aihara, Determination of iron(II) and total iron in environmental water samples by flow injection analysis with column preconcentration of chelating resin functionalized with N-hydroxyethylethylenediamine ligands and chemiluminescence detection, Talanta 49 (1999) 1059-1067. DOI: 10.1016/S0039-9140(99)00061-2.

[14] A. Huberman, C. Perez, Nonheme iron determination, Anal. Biochem. 307 (2002) 375-378. DOI: 10.1016/S0003-2697(02)00047-7.

[15] S. Zareba, H. Hopkala, Spectrophotometric determination of Fe(III) in pharmaceutical multivitamin preparations by azo dye derivatives of pyrocatechol, J. Pharm. Biol. Anal. 14 (1996) 1351-1354. DOI: 10.1016/S0731-7085(95)01735-6.

[16] S. S. Yamamura, J. H. Sikes, Use of Citrate-EDTA Masking for Selective Determination of Iron with 1,10-Phenanthroline, Anal. Chem. 38 (1966) 793-795. DOI: 10.1021/ac60238a037.

[17] G. F. Lee, W. Stumm. Determination of ferrous iron in the presence of ferric iron with Bathophenanthroline, J. Am, Water Works Assoc. 52 (1960) 1567-1574.

[18] L. L. Stookey, Ferrozine---a new spectrophotometric reagent for iron, Anal. Chem. 42 (1970) 779-781. DOI: 10.1021/ac60289a016.

[19] M. Morine, J. P. Scharff, La chelation des ions fer(III) par l'acide

pyrocatecholdisulfonique-3,5., Anal. Chim. Acta. 60 (1972) 101-108. DOI: 10.1016/S0003-2670(01)81888-2.

[20] I. Mori, M. Toyoda, Y. Fujita, T. Matsuo, K. Taguchi, Preconcentration of 1-(2-pyridylazo)—2-naphthol—iron(III)-capriquat on a membrane filter, and third-derivative spectrophotometric determination of iron(III), Talanta 41 (1994) 251-254. DOI: 10.1016/0039-9140(94)80116-9.

[21] D. Y. Yegorov, A. V. Kozlov, O. A. Azizova, Y. A. Vladimirov, Simultaneous determination of Fe(III) and Fe(II) in water solutions and tissue homogenates using desferal and 1,10-phenanthroline, Free Radic. Biol. Med. 15 (1993) 565-574. DOI: 10.1016/0891-5849(93)90158-Q.

[22] Z. Yi, G. Zhuang, P. R. Brown. R. A. Duce, High-performance liquid chromatographic method for the determination of ultratrace amounts of iron(II) in aerosols, rainwater, and seawater, Anal. Chem. 64 (1992) 2826-2830. DOI: 10.1021/ac00046a028.

[23] H. Bagheri, A. Gholami, A. Najafi, Simultaneous preconcentration and speciation of iron(II) and iron(III) in water samples by 2-mercaptobenzimidazole-silica gel sorbent and flow injection analysis system, Anal Chim. Acta. 424 (2000) 233-242. DOI: 10.1016/S0003-2670(00)01151-X.

[24] C. I. Measures, J. Yuan, J. A. Resing, Determination of iron in seawater by flow injection analysis using in-line preconcentration and spectrophotometric detection, Mar. Chem. 50 (1995) 3-12. DOI: 10.1016/0304-4203(95)00022-J.

[25] D. A. Skoog, D. M. West, F. J. Holler. Fundamentos de Química Analítica, 4ª ed. (1997), Reverte, Barcelona.

[26] L.F. Capitán-Vallvey, N. López-Ruiz, A. Martínez-Olmos, M.M. Erenas, A.J. Palma, Recent developments in computer vision-based analytical chemistry: A tutorial review, Anal Chim Acta. 899 (2015) 23-56. DOI: 10.1016/j.aca.2015.10.009.

[27] T. Yamamoto, H. Takiwaki, S. Arase, H. Ohshima, Derivation and clinical application of special imaging by means of digital cameras and Image J freeware for quantification of erythema and pigmentation, Skin Res. Technol. 14 (2008) 26-34. DOI: 10.1111/j.1600-0846.2007.00256.x.

[28] S. Schlücker, M. D. Schaeberle, S. W. Huffman, I. W. Levin, Raman Microspectroscopy: A Comparison of Point, Line, and Wide-Field Imaging Methodologies, Anal. Chem. 75 (2003) 4312-4318. DOI: 10.1021/ac034169h.

[29] T. Goldmann, A. Zyzik, S. Loeschke, W. Lindsay, E. Vollmer, Cost-effective gel documentation using a web-cam, J. Biochem. Biophys. Meth. 50 (2001) 91-95. DOI: 10.1016/S0165-022X(01)00174-9.

[30] G. Y. Fan, M. H. Ellisman, Digital imaging in transmission electron microscopy, J. Microsc. 200 (2000) 1-13. DOI: 10.1046/j.1365-2818.2000.00737.x.

[31] W.S. Lyra, V.B. dos Santos, A.G.G. Dionízio, V.L. Martins, L.F. Almeida, E. N. N. Gaião, P. H. G. D. Diniz, E.C. Silva, M.C.U. Araujo, Digital image-based flame emission spectrometry, Talanta 77 (2009) 1584-1589. DOI: 10.1016/j.talanta.2008.09.057.

[32] Q.S. Hanley, C. W. Earle, F. M. Pennebaker, S. P. Madden, M. B. Denton, Charge-Transfer Devices in Analytical Instrumentation, Anal. Chem. 68 (1996) 661A-667A. DOI: 10.1021/ac9621229.

[33] D. W. Koppenaal, C.J. Barinaga, M.B.B. Denton, R.P. Sperline, G.M. Hieftje, G.D. Schilling, F.J. Andrade, J.H. Barnes, MS Detectors, Anal. Chem. 77 (2005) 418A-427A. DOI: 10.1021/ac053495p.

[34] S. Merk, A. Lietz, M. Kroner, M. Valler, R. Heilker, Time-Resolved Fluorescence Measurements Using Microlens Array and Area Imaging Devices, Comb. Chem. High Throughput Screen 7 (2004) 45-54. DOI: 10.2174/138620704772884814.

[35] B. Chakravarti, M. Loie, W. Ratanaprayul, A. Raval, S. Gallagher, D. N. Chakravarti, A highly uniform UV transillumination imaging system for quantitative analysis of nucleic acids and proteins, Proteomics 8 (2008) 1789-1797. DOI: 10.1002/pmic.200700891.

[36] E. Galindo, C.P. Larralde-Corona, T. Brito, M.S. Córdova-Aguilar, B. Taboada, L. Vega-Alvarado, G. Corkidi, Development of advanced image analysis techniques for the in situ characterization of multiphase dispersions occurring in bioreactors, J. Biotechnol. 116 (2005) 261-270. DOI: 10.1016/j.jbiotec.2004.10.018.

[37] D. P. Mesquita, O. Dias, A.L. Amaral, E.C. Ferreira, Monitoring of activated sludge settling ability through image analysis: validation on full-scale wastewater treatment plants, Bioprocess Biosyst. Eng. 32 (2009) 361-367. DOI: 10.1007/s00449-008-0255-z.

[38] M.D. Lancaster, M. Goodall, E. T. Bergström, S. McCrossen, P. Myers, Quantitative measurements on wetted thin layer chromatography plates using a charge coupled device camera, J. Chromatogr. A. 1090 (2005) 165-171. DOI: 10.1016/j.chroma.2005.06.068.

[39] M.D. Lancaster, M. Goodall, E. T. Bergström, S. McCrossen, P. Myers, Real-Time Image Acquisition for Absorbance Detection and Quantification in Thin-Layer Chromatography, Anal. Chem. 78 (2006) 905-911. DOI: 10.1021/ac051390g.

[40] T. Hayakawa, M. Hirai, An Assay of Ganglioside Using Fluorescence Image Analysis on a Thin-Layer Chromatography Plate, Anal. Chem. 75 (2003) 6728-6731. DOI: 10.1021/ac0346095.

[41] M. Prosek, I. Vovk, Reproducibility of densitometric and image analysing quantitative evaluation of thin-layer chromatograms, J. Chromatogr. A. 779 (1997) 329-336. DOI: 10.1016/S0021-9673(97)00442-1.

[42] J.W. Wagner, G.M. Miskelly, Background correction in forensic photography. I. Photography of blood under conditions of non-uniform illumination or variable substrate color-theoretical aspects and proof of concept, J. Forensic Sci. 48 (2003) 593-603. DOI: 10.1520/JFS2002303.

[43] J.W. Wagner, G.M. Miskelly, Background Correction in Forensic Photography II. Photography of Blood Under Conditions of Non-Uniform Illumination or Variable Substrate Color-Practical Aspects and Limitations, J. Forensic Sci. 48 (2003) 604-613. DOI: 10.1520/JFS2002408.

[44] A.V.I. Hess, Digitally Enhanced Thin-Layer Chromatography: An Inexpensive, New Technique for Qualitative and Quantitative Analysis, J. Chem. Ed. 84 (2007) 842-847. DOI: 10.1021/ed084p842.

[45] T. Cumberbatch, T. Q. S. Hanley, Quantitative Imaging in the Laboratory: Fast Kinetics and Fluorescence Quenching, J. Chem. Ed. 84 (2007) 1319-1322.

DOI: 10.1021/ed084p1319.

[46] E.N. Gaiao, V.L. Martins, W.S. Lyra, L.F. Almeida, E.C. Silva, M.C.U. Araujo, Digital image-based titrations, Anal. Chim. Acta 570 (2006) 283–290. DOI: 10.1016/j.aca.2006.04.048.

[47] A. Alimelli, D. Filippini, R. Paolesse, S. Moretti, G. Ciolfi, A, D'Amico, I. Lundstrom, C. Di Natale, Direct quantitative evaluation of complex substances using computer screen photo-assisted technology: The case of red wine, Anal. Chim. Acta 597 (2007) 103-112. DOI: 10.1016/j.aca.2007.06.033.

[48] A.W. Martinez, S.T. Phillips, E. Carrilho, S.W. Thomas, H. Sindi, G.M. Whitesides, Simple Telemedicine for Developing Regions: Camera Phones and Paper-Based Microfluidic Devices for Real-Time, Off-Site Diagnosis, Anal. Chem. 80 (2008) 3699-3707. DOI: 10.1021/ac800112r.

[49] D. J. Soldat, P. Barak, B. J. Lepore, Microscale Colorimetric Analysis Using a Desktop Scanner and Automated Digital Image Analysis, J. Chem. Educ. 86 (2009) 617-620. DOI: 10.1021/ed086p617.

[50] K.R. Mathews, J.D. Landmark, D.F. Stickle, Quantitative Assay for Starch by Colorimetry Using a Desktop Scanner, J. Chem. Educ. 81 (2004) 702-704. DOI: 10.1021/ed081p702.

[51] B. Cochran, D. Lunday, F. Miskevich, Kinetic Analysis of Amylase Using Quantitative Benedict's and Iodine Starch Reagents, J. Chem Educ. 85 (2008) 401-403. DOI: 10.1021/ed085p401.

[52] M. Kompany-Zareh, S. Mirzaei, Genetic algorithm-based method for selecting conditions in multivariate determination of povidone-iodine using hand scanner, Anal. Chim. Acta 521 (2004) 231-236. DOI: 10.1016/j.aca.2004.05.067.

[53] M. Kompany-Zareh, M. Mansourian, F. Ravaee, Simple method for colorimetric spot-test quantitative analysis of Fe(III) using a computer controlled hand-scanner, Anal. Chim. Acta 471 (2002) 97-104. DOI: 10.1016/S0003-2670(02)00871-1.

[54] L. Lahuerta, P. Alemán, G. M. Antón, R. Martín, A. M. Mellado, J. Martínez, Quantitative colorimetric-imaging analysis of nickel in iron meteorites, Talanta 83 (2011) 1575-1579. DOI: 10.1016/j.talanta.2010.11.058.

[55] L. Lahuerta, A. M. Mellado, J. Martínez, Quantitative Colorimetric Analysis of Some Inorganic Salts Using Digital Photography, Anal. Lett. 44 (2011) 1674-1682. 10.1080/00032719.2010.520394.

[56] Farmacopea de los Estados Unidos (USP), 23ª ed. (1995), The United State Pharmacopeial Convention USP, Rockville.

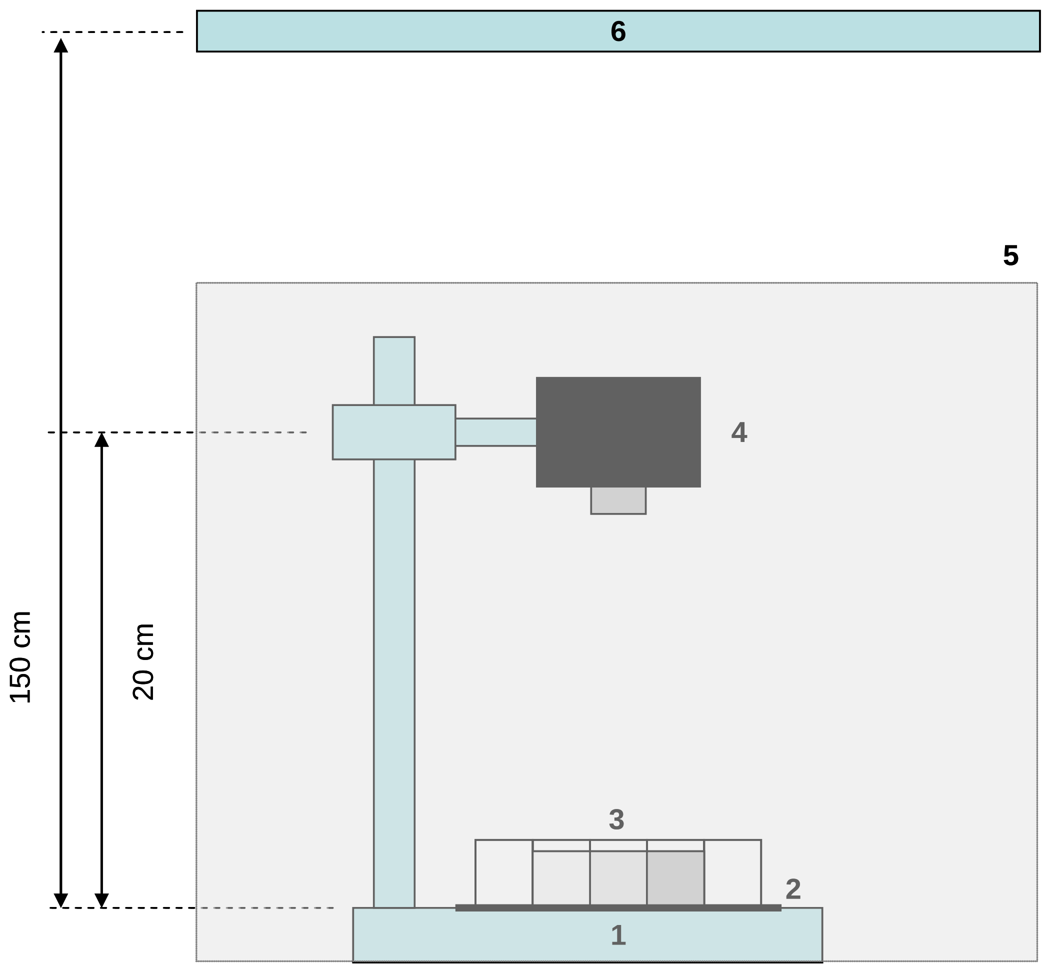

Fig. 1. Equipment used to obtain digital images with a photographic camera (4). Support (1), black cardboard (2), spot plate (3), white methacrylate box (5) and fluorescent strips (6).

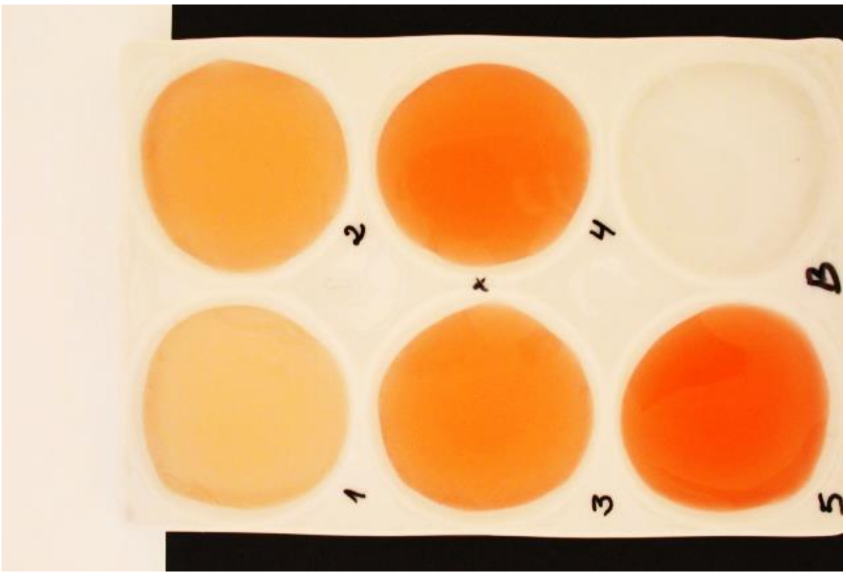

Fig. 2a. Spot plate filled with standard solutions and strip of white paper on its left.

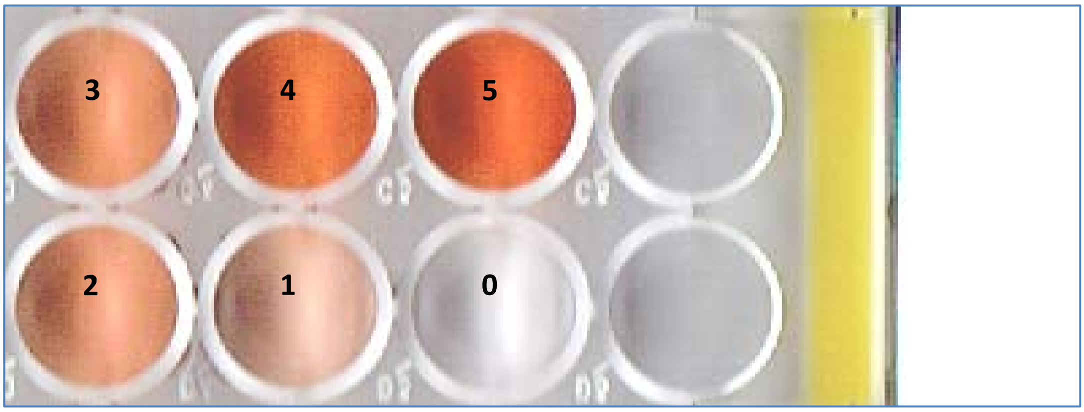

Fig. 2b. Microplate filled with standard solutions containing variable concentrations of Fe (II) (mg L^{-1}) and strip of white paper on its right.

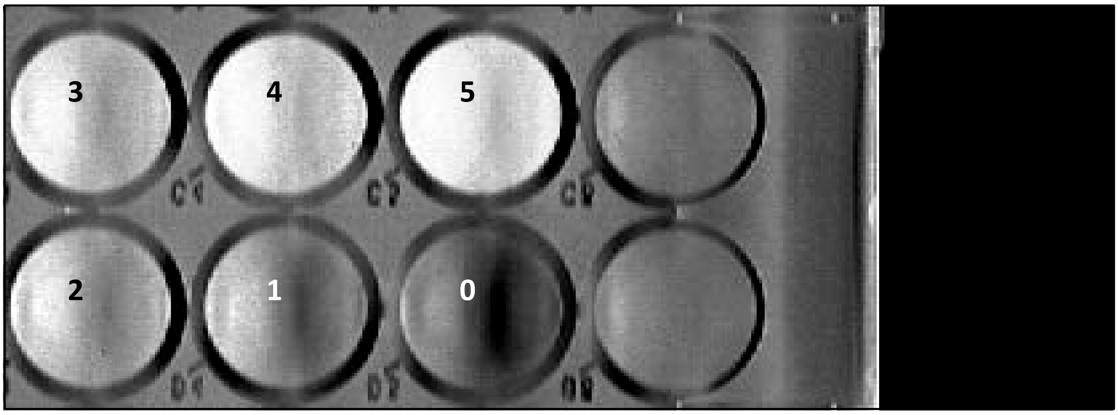

Fig. 2c. Microplate filled with standard solutions containing variable concentrations of Fe (II) (mg L^{-1}) and the sample (S), and strip of white paper on its right (inverted image).

Table 1
Slopes and coefficients of determination of the calibration curves obtained at different exposure times.

Exposure time / s	Slope	r^2
1/4	0,0043	0,9949
1/8	0,0571	0,9990
1/15	0,0694	0,9975
1/30	0,0924	0,9968

Table 2
Slopes and coefficients of determination of the calibration curves obtained at different apertures (F) and exposure times, and standard deviation of the slope (N = 3).

Exposure time / s	F	Slope	r^2	Standard deviation
1/2	8,4	0,0668	0,9997	0,0004
1/4	6	0,0691	0,9995	0,0005
1/8	4,2	0,0676	0,9995	0,0008
1/15	3	0,0719	0,9987	0,0007

Table 3
Mean values (N = 3) obtained with the five desktop scanners compared.

Scanner	RGB channel	Slope (ROI: 4500 pixels)	r^2 (ROI: 4500 pixels)	Slope (ROI: 50 pixels)	r^2 (ROI: 50 pixels)
ACER	Green	9.9	0.9754	14.0	0.9729
S2W 3300V	Blue	14.0	0.953	19.9	0.9615
BROTHER	Green	14.2	0.947	17.9	0.9782
DCP-J132W*	Blue	16.5	0.8933	24.7	0.9406
HP 1510	Green	10.9	0.9583	19.9	0.9726
	Blue	10.2	0.92476	15.7	0.9756
HP 3100	Green	4.5	0.9836	6.8	0.9488
	Blue	7.8	0.9909	10.8	0.9652
HP 4300	Green	7.9	0.9853	11.6	0.9917
	Blue	14.0	0.9819	17.1	0.9862

* The values for the Brother DCP-J132W scanner were measured at 2500 pixels rather than 4500 because its images were of lower resolution.

Table 4
Influence of the amount of Gaussian blur applied to an image (green channel) with two circular regions of interest (ROI) of different size.

Gaussian blur	**Calibration curve (ROI: 2500 pixels)**	**Calibration curve (ROI: 50 pixels)**
0	$y = 14.097x + 148.77$ $r^2 = 0.9539$	$y = 18.343x + 108.57$ $r^2 = 0.9569$
2.5	$y = 13.087x + 150.03$ $r^2 = 0.9367$	$y = 18.043x + 112.06$ $r^2 = 0.9579$
5	$y = 13.453x + 145.69$ $r^2 = 0.9567$	$y = 17.8x + 117.16$ $r^2 = 0.9608$
7.5	$y = 12.51x + 143.9$ $r^2 = 0.9624$	$y = 16.988x + 124.33$ $r^2 = 0.957$
10	$y = 11.154x + 144.42$ $r^2 = 0.9596$	$y = 16.154x + 126.88$ $r^2 = 0.978$

Table 5
Analytical figures of merit of the proposed methods.

Parameter	**Digital camera**	**Desktop scanner**
Slope	0.067	29.886
Origin of straight (y-intercept)	0.141	9.381
r^2	0.999	0.995
Standard deviation of blank	0.008	1.999
CLD (empirical CLD) / mg L^{-1}	0.36 (0.2-0.4)	0.2 (0.4-0.6)
CLQ / mg L^{-1}	1.18	0.70
Within-day reproducibility / %	3.0 (*N*=5)	3.6 (*N*=5)
Between-day reproducibility / %	4.0	4.6

Table 6
Results for the quantification of Fe (in mg per capsule) for real samples, using the four analytical methods, as an average of three samples processed independently.

Real sample	**Cerimetry**	**SP***	**Desktop scanner**	**Digital camera**
Ferbisol®	101 ± 1	104 ± 5	102 ± 3	103 ± 5
Ferro sanol®	103 ± 1	103 ± 3	103 ± 2	103± 3

SP = spectrophotometry.